

# Quantum information and triangular optical lattices\*

Alastair Kay,<sup>1</sup> Derek K. K. Lee,<sup>2</sup> Jiannis K. Pachos,<sup>1</sup> Martin B. Plenio,<sup>2</sup> Moritz E. Reuter,<sup>2</sup> and Enrique Rico<sup>3</sup>

<sup>1</sup>*Department of Applied Mathematics and Theoretical Physics,  
University of Cambridge, Cambridge CB3 0WA, UK,*

<sup>2</sup>*Blackett Laboratory, Imperial College, London SW7 2BW, UK,*

<sup>3</sup>*Department d'Estructura i Constituents de la Matèria,  
Universitat de Barcelona, 08028, Barcelona, Spain.*

(Dated: July 25, 2018)

The regular structures obtained by optical lattice technology and their behaviour are analysed from the quantum information perspective. Initially, we demonstrate that a triangular optical lattice of two atomic species, bosonic or fermionic, can be employed to generate a variety of novel spin-1/2 models that include effective three-spin interactions. Such interactions can be employed to simulate specific one or two dimensional physical systems that are of particular interest for their condensed matter and entanglement properties. In particular, connections between the scaling behaviour of entanglement and the entanglement properties of closely spaced spins are drawn. Moreover, three-spin interactions are well suited to support quantum computing without the need to manipulate individual qubits. By employing Raman transitions or the interaction of the atomic electric dipole moment with magnetic field gradients, one can generate Hamiltonians that can be used for the physical implementation of geometrical or topological objects. This work serves as a review article that also includes many new results.

PACS numbers: 03.75.Kk, 05.30.Jp, 42.50.-p, 73.43.-f

## I. INTRODUCTION

With the development of optical lattice technology [1, 2, 3], considerable attention has been focused on the realisation of quantum computation [4, 5, 6, 7] as well as quantum simulation of a variety of many-particle systems, such as spin chains and lattices [8, 9, 10, 11]. This technology provides the possibility to probe and realise complex quantum models with unique properties in the laboratory. Examples that are of interest in various areas of physics are systems that include many-body interactions. These have been hard to study in the past due to the difficulty in controlling them externally and isolating them from the environment [12]. To overcome these problems, techniques have been developed in quantum optics [13, 14, 15] which minimise imperfections and impurities in the implementation of the desired structures, thus paving the way for the consideration of such “higher order” phenomena of multi-particle interactions. Their applications are of much interest to cold atom technology as well as to condensed matter physics and quantum information, some of which we shall see here.

The initial point of our study is the presentation of the rich dynamics that governs the behaviour of an ultra cold atomic ensemble when it is superposed with appropriate optical lattices. For this purpose we consider the case of two species of atoms, denoted here by  $\uparrow$  and  $\downarrow$  (see [8, 9, 11]), trapped in the potential minima of a periodic lattice. These species can be two different hyperfine ground states of the same atom, coupled, via an excited

state, by a Raman transition. The system is brought initially into the Mott insulator phase where the number of atoms at each site of the lattice is well defined. By restricting to the case of only one atom per site, it is possible to characterise the system by pseudo-spin basis states provided by the internal ground states of the atom. Interactions between atoms in different sites are facilitated by virtual transitions. These are dictated by the tunneling coupling,  $J$ , from one site to its neighbours and by collisional couplings,  $U$ , that take place when two or more atoms are within the same site. Eventually the evolution of the system can be effectively described by a wide set of spin interactions with coupling coefficients completely controlled by the tunneling and collisional couplings. This gives rise to the consideration of several applications that are mainly related with the three-spin interactions simulated on the lattice, which is the main focus of the present article.

In that spirit, implementation of quantum simulation, of different physical models can be realised, with ground states that present a rich structure, such as multiple degeneracies and a variety of quantum phase transitions [16, 17, 18]. Some of these multi-spin interactions have been theoretically studied in the past in the context of the hard rod boson [19, 20, 21], using self-duality symmetries [22, 23]. Phase transitions between the corresponding ground states have been analysed [24, 25]. Subsequently, these phases may also be viewed as possible phases of the initial system, in the Mott insulator, where the behaviour of its ground state can be controlled at will [26]. In this context the so-called cluster Hamiltonian is of considerable interest as its ground state exhibits unique entanglement properties. In this article we review the status quo of the existing analysis of these entanglement

---

\*Based on talk presented by J. K. Pachos at CEWQO 2004.

properties as well as presenting new results that indicate interesting links between the entanglement properties of closely spaced spins and the scaling of entanglement with spin separation.

To implement quantum computing, one can take advantage of the three-spin interaction to construct multi-qubit gates that eventually can lead to quantum computation without the need to manipulate single qubits, referred to as ‘global addressing’. We use a single qubit to localise operations, meaning that one and two qubit gates in a typical quantum computing scheme are replaced by two and three qubit gates in this scheme, which is what makes a triangular lattice with three-spin interactions such a natural environment for implementation of this concept. This global addressing lifts the stringent experimental requirement of single atom addressing for performing quantum gates. Moreover, error correction can be performed without the need to make measurements during the computation.

The paper is organised as follows. In Section II, we present the physical system and the conditions required to obtain three-body interactions. The effective three-spin Hamiltonians for the case of bosonic or fermionic species of atoms in a system of three sites on a lattice are given in Sec. III. In Sec. IV we introduce complex couplings by considering the effect Raman transitions can have on the tunneling process and generalised effective Hamiltonians are presented that do not preserve the number of atoms of each species. In addition, the electric dipole of the atoms is considered which, through interaction with an external inhomogeneous field, can generate chirality. In Sec. VI a variety of entanglement properties of spin chains with three-spin interactions is analysed, and the cluster Hamiltonian is presented along with novel connections between the scaling behaviour of entanglement and the entanglement properties of closely spaced spins. A global addressing quantum computation model is presented in Sec. VII and, finally, in Sec. VIII concluding remarks are given.

## II. THE PHYSICAL MODEL

Let us consider a cloud of ultra cold neutral atoms superimposed with several optical lattices [8, 9, 10, 11, 27]. For sufficiently strong intensities of the laser field, this system can be placed in the Mott insulator phase where the expectation value of only one particle per lattice site is energetically allowed [3]. This still allows for the implementation of non-trivial manipulations by virtual transitions that include energetically unfavourable states. Here, we are particularly interested in the setup of lattices that form an equilateral triangular configuration, as shown in Fig. 1. This allows for the simultaneous superposition of the positional wave functions of the atoms belonging to the three sites. As we shall see in the following, this results in the generation of a three-spin interaction.

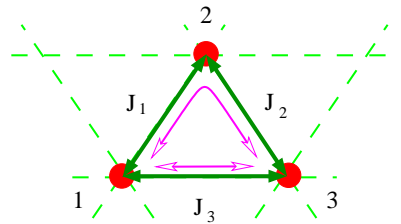


FIG. 1: The basic building block for the triangular lattice configuration. Three-spin interaction terms appear between sites 1, 2 and 3. For example, tunneling between 1 and 3 can happen through two different paths, directly and through site 2. The latter results in an exchange interaction between 1 and 3 that is influenced by the state of site 2.

The main contributions to the dynamics of the atoms in the lattice sites are given by the collisions of the atoms within the same site and the tunneling transitions of the atoms between neighbouring sites. In particular, the coupling of the collisional interaction for atoms in the same site are taken to be very large in magnitude, while they are supposed to vanish when they are in different sites. Due to the low temperature of the system, this term is completely characterised by the s-wave scattering length. Furthermore, the overlap of the Wannier wave functions between adjacent sites determines the tunneling amplitude,  $J$ , of the atoms from one site to its neighbours. Here, the relative rate between the tunneling and the collisional interaction term is supposed to be very small, i.e.  $J \ll U$ , so that the state of the system is mainly dominated by the collisional interaction.

The Hamiltonian describing the three lattice sites with three atoms of species  $\sigma = \{\uparrow, \downarrow\}$  subject to the above interactions is given by

$$H = H^{(0)} + V, \quad (2.1)$$

with

$$H^{(0)} = \frac{1}{2} \sum_{i\sigma\sigma'} U_{\sigma\sigma'} a_{i\sigma}^\dagger a_{i\sigma'}^\dagger a_{i\sigma'} a_{i\sigma},$$

$$V = - \sum_{j\sigma} (J_j^\sigma a_{j\sigma}^\dagger a_{j+1\sigma} + \text{H.c.}),$$

where H.c. denotes the Hermitian conjugate, and  $a_{j\sigma}$  denotes the annihilation operator of atoms of species  $\sigma$  at site  $j$ . The annihilation operator can describe fermions or bosons, satisfying commutation or anticommutation relations respectively, given by

$$[a_{j\sigma}, a_{j'\sigma'}^\dagger]_{\pm} = \delta_{jj'} \delta_{\sigma\sigma'}, \quad (2.2)$$

$$[a_{j\sigma}, a_{j'\sigma'}^\dagger]_{\pm} = [a_{j\sigma}^\dagger, a_{j'\sigma'}^\dagger]_{\pm} = 0,$$

where the  $\pm$  sign denotes the anticommutator or the commutator. The Hamiltonian  $H^{(0)}$  is the lowest order in the expansion with respect to the tunneling interaction.

Due to the large collisional couplings, activated when two or more atoms are present within the same site, the

weak tunneling transitions do not change the average number of atoms per site. This is achieved by adiabatic elimination of higher population states during the evolution, leading to an effective Hamiltonian [28]. The latter allows virtual transitions between these levels providing eventually non-trivial evolutions. According to this the low energy evolution of the bosonic or fermionic system, up to the third order in the tunneling interaction, is given by the effective Hamiltonian

$$H_{\text{eff}} = - \sum_{\gamma} \frac{V_{\alpha\gamma} V_{\gamma\beta}}{E_{\gamma}} + \sum_{\gamma\delta} \frac{V_{\alpha\gamma} V_{\gamma\delta} V_{\delta\beta}}{E_{\gamma} E_{\delta}} + \mathcal{O}\left(\frac{J^4}{U^3}\right). \quad (2.3)$$

The indices  $\alpha, \beta$  refer to states with one atom per site while  $\gamma, \delta$  refer to states with two or more atomic populations per site,  $E_{\gamma}$  are the eigenvalues of the collisional part,  $H^{(0)}$ , while we neglected fast rotating terms which is effective for long time intervals [28].

It is instructive to estimate the energy scales involved in such a physical system. We would like to have a significant effect of the three-spin interaction within the decoherence times of the experimental system, which we can take here to be of the order of a few tens of ms. It is possible to vary the tunneling interactions from zero to some maximum value which we can take here to be of the order of  $J/\hbar \sim 1$  kHz [2]. In order to have a significant effect from the term  $J^3/U^2$  within the decoherence time, one should choose  $U/\hbar \sim 10$  kHz. This can be achieved experimentally by moving close to a Feshbach resonance [29, 30, 31], where  $U$  can take significantly large values. With respect to these parameters we have  $J/U \sim 10^{-1}$ , which is within the Mott insulator regime, while the next order in perturbation theory is an order of magnitude smaller than the one considered here and hence negligible. This places the requirements of our proposal for detecting the effect of three-spin interactions within the range of the possible experimental values of the state of the art technology.

### III. THE EFFECTIVE THREE-SPIN INTERACTIONS

The perturbative dynamics of the system is better presented in terms of effective spin interactions. Indeed, within the regime of single atom occupancy per site, it is possible to switch to the pseudo-spin basis of states of the site  $j$  given by  $|\uparrow\rangle \equiv |n_{j\uparrow} = 1, n_{j\downarrow} = 0\rangle$  and  $|\downarrow\rangle \equiv |n_{j\uparrow} = 0, n_{j\downarrow} = 1\rangle$ . Hence, the effective Hamiltonian can be given in terms of Pauli matrices acting on states expressed in the pseudo-spin basis, as we shall see in the following.

#### A. The bosonic model

In this subsection and the following one, we will develop the Mott-Hubbard model in perturbation theory

up to third order in  $J/U$ , i.e. the ratio of the tunneling rate to the interaction term. In the first case, we will study a bosonic system, when two atoms of the same species are allowed to be in the same state. Eventually, our model is described by

$$H_{\text{eff}} = \sum_{j=1}^3 \left[ A_j \mathbb{1} + B_j \sigma_j^z + \lambda_j^{(1)} \sigma_j^z \sigma_{j+1}^z + \lambda_j^{(2)} (\sigma_j^x \sigma_{j+1}^x + \sigma_j^y \sigma_{j+1}^y) + \lambda_j^{(3)} \sigma_j^z \sigma_{j+1}^z \sigma_{j+2}^z + \lambda_j^{(4)} (\sigma_j^x \sigma_{j+1}^z \sigma_{j+2}^x + \sigma_j^y \sigma_{j+1}^z \sigma_{j+2}^y) \right], \quad (3.1)$$

where  $\sigma_j^{\alpha}$  is the  $\alpha$  Pauli matrix at the site  $j$ . The couplings  $A, B$ , and  $\lambda^{(i)}$ , are given in terms of  $J^{\sigma}/U_{\sigma\sigma'}$  by

$$\begin{aligned} A_j &= - J_1^{\uparrow} J_2^{\uparrow} J_3^{\uparrow} \left( \frac{9}{2U_{\uparrow\uparrow}^2} + \frac{3}{2U_{\uparrow\downarrow}^2} + \frac{3}{U_{\uparrow\downarrow} U_{\uparrow\uparrow}} \right) - \\ &\quad J_j^{\uparrow 2} \left( \frac{1}{U_{\uparrow\uparrow}} + \frac{1}{2U_{\uparrow\downarrow}} \right) + (\uparrow\leftrightarrow\downarrow), \\ B_j &= - \frac{J_j^{\uparrow 2} + J_{j+2}^{\uparrow 2}}{U_{\uparrow\uparrow}} - \frac{J_1^{\uparrow} J_2^{\uparrow} J_3^{\uparrow}}{U_{\uparrow\uparrow}} \left( \frac{1}{U_{\uparrow\downarrow}} + \frac{9}{2U_{\uparrow\uparrow}} \right) - \\ &\quad (\uparrow\leftrightarrow\downarrow), \\ \lambda_j^{(1)} &= - J_1^{\uparrow} J_2^{\uparrow} J_3^{\uparrow} \left( \frac{9}{2U_{\uparrow\uparrow}^2} - \frac{1}{2U_{\uparrow\downarrow}^2} - \frac{1}{U_{\uparrow\downarrow} U_{\uparrow\uparrow}} \right) - \\ &\quad J_j^{\uparrow 2} \left( \frac{1}{U_{\uparrow\uparrow}} - \frac{1}{2U_{\uparrow\downarrow}} \right) + (\uparrow\leftrightarrow\downarrow), \\ \lambda_j^{(2)} &= - J_j^{\downarrow} J_{j+1}^{\uparrow} J_{j+2}^{\uparrow} \left( \frac{3}{2U_{\uparrow\downarrow}^2} + \frac{1}{2U_{\uparrow\uparrow}^2} + \frac{1}{U_{\uparrow\downarrow} U_{\uparrow\uparrow}} \right) - \\ &\quad \frac{J_j^{\uparrow} J_j^{\downarrow}}{2U_{\uparrow\downarrow}} + (\uparrow\leftrightarrow\downarrow), \\ \lambda_j^{(3)} &= - \frac{J_1^{\uparrow} J_2^{\uparrow} J_3^{\uparrow}}{U_{\uparrow\uparrow}} \left( \frac{3}{2U_{\uparrow\uparrow}} - \frac{1}{U_{\uparrow\downarrow}} \right) - (\uparrow\leftrightarrow\downarrow), \\ \lambda_j^{(4)} &= - \frac{J_j^{\uparrow} J_{j+1}^{\uparrow} J_{j+2}^{\downarrow}}{U_{\uparrow\uparrow}} \left( \frac{1}{2U_{\uparrow\uparrow}} + \frac{1}{U_{\uparrow\downarrow}} \right) - (\uparrow\leftrightarrow\downarrow), \end{aligned} \quad (3.2)$$

where the symbol  $(\uparrow\leftrightarrow\downarrow)$  denotes the repeating of the same term as on its left, but with the  $\uparrow$  and  $\downarrow$  indices interchanged.

Knowing the dependence of the effective couplings allows us to modify the dynamics of the system at will, by changing the values of the tunneling rate or coupling constant, as seen in Fig. 2. Moreover, one body interactions in the Hamiltonian can be eliminated with an arbitrary Zeeman term of the form  $\sum_j \vec{B} \cdot \vec{\sigma}_j$  that can be added by applying a Raman transition with the appropriate laser fields. One can also isolate different parts of Hamiltonian (3.1), each one including a three-spin interaction term, by varying the tunneling and/or the collisional couplings appropriately so that particular terms in

(3.1) vanish, while others are freely varied. An example of this can be seen in Fig. 3 where the couplings  $\lambda^{(1)}$  and  $\lambda^{(3)}$  are depicted. There, for the special choice of the collisional terms,  $U_{\uparrow\uparrow} = U_{\downarrow\downarrow} = 2.12U_{\uparrow\downarrow}$ , the  $\lambda^{(1)}$  coupling is kept to zero for a wide range of the tunneling couplings, while the three-spin coupling,  $\lambda^{(3)}$ , can take any arbitrary value. One can also suppress the exchange interactions by keeping one of the two tunneling couplings zero, without affecting the freedom in obtaining arbitrary positive or negative values for  $\lambda^{(3)}$ , as seen in Fig. 3.

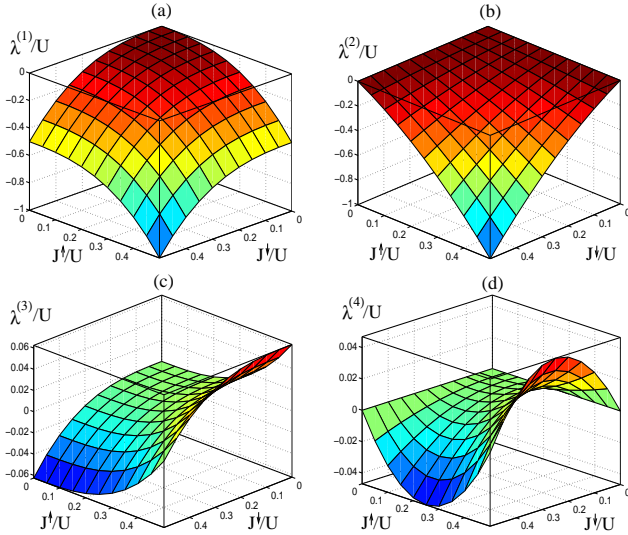


FIG. 2: The effective couplings (a)  $\lambda^{(1)}$ , (b)  $\lambda^{(2)}$ , (c)  $\lambda^{(3)}$  and (d)  $\lambda^{(4)}$  as functions of the tunneling couplings  $J^\uparrow/U$  and  $J^\downarrow/U$ . The tunneling couplings are set to be  $J_1^\uparrow = J_2^\uparrow = J_3^\uparrow$  and the collisional couplings to be  $U_{\uparrow\uparrow} = U_{\uparrow\downarrow} = U_{\downarrow\downarrow} = U$ . All the parameters are normalised with respect to  $U$ .

## B. The fermionic model

In this subsection, we will show the effective Hamiltonian for a system where two atoms of the same species are not allowed to be in the same site, so that they are described by fermionic operators. For the same reason, there is just one collisional coupling  $U_{\uparrow\downarrow} = U$ , and the others can be thought to contribute with an infinite energy,  $U_{\uparrow\uparrow}, U_{\downarrow\downarrow} \rightarrow \infty$ . After a tedious calculation and keeping terms to third order in  $J_i^\sigma/U$ , the effective Hamiltonian appears as,

$$H_{\text{eff}} = \sum_{j=1}^3 \left[ \mu_j^{(1)} (\mathbb{I} - \sigma_j^z \sigma_{j+1}^z) + \mu_j^{(3)} (\sigma_j^z - \sigma_1^z \sigma_2^z \sigma_3^z) + \mu_j^{(2)} (\sigma_j^x \sigma_{j+1}^x + \sigma_j^y \sigma_{j+1}^y) + \mu_j^{(4)} (\sigma_j^x \sigma_{j+1}^z \sigma_{j+2}^x + \sigma_j^y \sigma_{j+1}^z \sigma_{j+2}^y) \right],$$

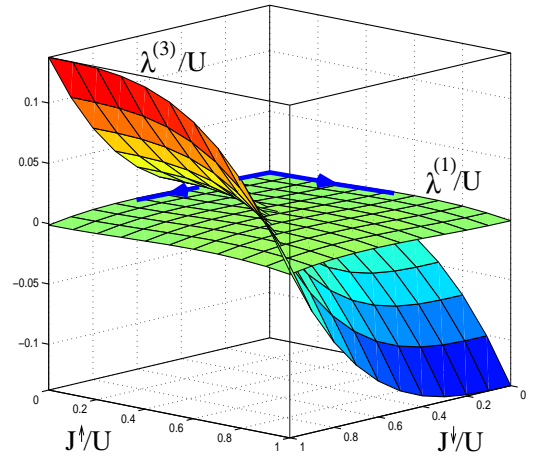


FIG. 3: The effective couplings  $\lambda^{(1)}$  and  $\lambda^{(3)}$  are plotted against  $J^\uparrow/U$  and  $J^\downarrow/U$  for  $U_{\uparrow\uparrow} = U_{\downarrow\downarrow} = 2.12U$  and  $U_{\uparrow\downarrow} = U$ . The coupling  $\lambda^{(1)}$  appears almost constant and zero as the unequal collisional terms can create a plateau area for a small range of the tunneling couplings, while  $\lambda^{(3)}$  can be varied freely to positive or negative values.

where the effective couplings are functions of the tunneling and collisional couplings, given by

$$\begin{aligned} \mu_j^{(1)} &= -\frac{1}{2U} (J_j^{\uparrow 2} + J_j^{\downarrow 2}), & \mu_j^{(2)} &= \frac{1}{U} J_j^\uparrow J_j^\downarrow, \\ \mu_j^{(3)} &= -\frac{1}{2U^2} (J_1^\uparrow J_2^\uparrow J_3^\uparrow - J_1^\downarrow J_2^\downarrow J_3^\downarrow), \\ \mu_j^{(4)} &= \frac{3}{2U^2} (J_j^\uparrow J_{j+1}^\uparrow J_{j+2}^\downarrow - J_j^\downarrow J_{j+1}^\downarrow J_{j+2}^\uparrow). \end{aligned}$$

In this case, the dependence of the coupling terms on the parameters of the initial Hamiltonian is simpler than in the bosonic one. If the tunneling constants do not depend on the pseudo-spin orientation, indicated here by the subscript  $j = 1, 2, 3$ , then any three-spin interaction vanishes. Nevertheless, when the tunneling amplitudes depend on the spin and there is just one of the orientation with non-zero tunneling, then, only the two- and three-spin interactions in the  $z$  direction remain. A general picture of their behaviour can be seen in Fig. 4.

## IV. COMPLEX COUPLINGS

### A. Raman activated tunneling

From the previous models, it is possible to create new, different, Hamiltonians by employing techniques available from quantum optics [8, 11, 32], like the application of Raman transitions during the tunneling process. If the lasers producing the Raman transition form standing waves, it is possible to activate tunneling transitions of atoms that simultaneously experience a change in their

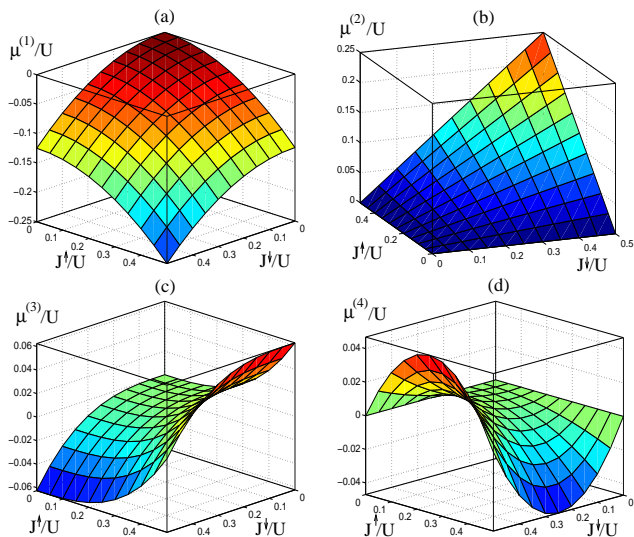


FIG. 4: The effective couplings (a)  $\mu^{(1)}$ , (b)  $\mu^{(2)}$ , (c)  $\mu^{(3)}$  and (d)  $\mu^{(4)}$  as functions of the tunneling couplings  $J^\uparrow/U$  and  $J^\downarrow/U$ , where the tunneling couplings are set to be  $J_1^\sigma = J_2^\sigma = J_3^\sigma$ .

internal state. As we shall see in the following, the resulting Hamiltonian is given by an  $SU(2)$  rotation applied to each Pauli matrix of the previous Hamiltonians.

Consider the case of activating the tunneling with the application of two individual Raman transitions. These transitions consist of four paired laser beams  $L_1, L_2$  and  $L'_1, L'_2$ , each pair having a blue de-tuning  $\Delta$  and  $\Delta'$ , different for the two different transitions. The phases and amplitudes of the laser beams can be properly tuned so that the Raman transitions allow the tunneling of the states

$$\begin{aligned} |+\rangle &\equiv \cos\theta|a\rangle + \sin\theta e^{-i\phi}|b\rangle \\ |-\rangle &\equiv \sin\theta|a\rangle - \cos\theta e^{-i\phi}|b\rangle, \end{aligned}$$

or in a compact notation,

$$\begin{pmatrix} |+\rangle \\ |-\rangle \end{pmatrix} = g(\phi, \theta) \begin{pmatrix} |a\rangle \\ |b\rangle \end{pmatrix} \quad (4.1)$$

with the unitary  $SU(2)$  matrix

$$g(\phi, \theta) = \begin{pmatrix} \cos\theta & e^{i\phi} \sin\theta \\ \sin\theta & -e^{i\phi} \cos\theta \end{pmatrix} \quad (4.2)$$

In the above equations,  $\phi$  denotes the phase difference between the  $L_i$  laser field, while  $\tan\theta = |\Omega_2/\Omega_1|$ .  $\Omega_i$  are the Rabi frequencies of the laser fields. Hence, the resulting tunneling Hamiltonian can be obtained from the initial one via an  $SU(2)$  rotation,

$$V_c = gVg^\dagger = -\sum_i (J_+ c_i^{+\dagger} c_{i+1}^+ + J_- c_i^{-\dagger} c_{i+1}^- + \text{H.c.}).$$

where the corresponding tunneling couplings are formally identified, i.e.  $J^+ = J^\uparrow$  and  $J^- = J^\downarrow$ . Note that the collisional Hamiltonian is not affected by the Raman transitions, and hence it is not transformed under  $g$  rotations.

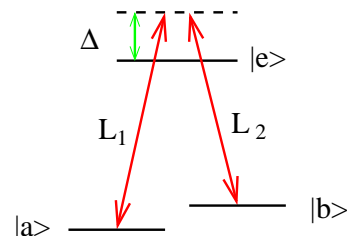


FIG. 5: Example of a Raman transition activated by a pair of blue detuning laser fields  $L_1$  and  $L_2$ .

It is easy to derive the effective Hamiltonian for this transformation using the perturbative expansion. From (2.3) we straightforwardly obtain the second, third and, likewise, any order term of the Hamiltonian  $\tilde{H}_{\text{eff}}$  that appear after the application of the Raman transition. They are given by an  $SU(2)$  rotation that acts on the Pauli matrices of the initial effective Hamiltonian and read

$$\tilde{H}_{\text{eff}}^{(n)}(\phi, \theta) = g(\phi, \theta) H_{\text{eff}}^{(n)} g^\dagger(\phi, \theta),$$

where  $n$  is the order of the perturbation.

This approach provides a variety of control parameters (e.g. the angle  $\phi$  and the ratio of the couplings of the two added Hamiltonians) and, in addition, one can have these variables independent for each of the three directions of the two dimensional (triangular) optical lattice. Particular settings of these structures have been proved to generate topological phenomena [11] that support exotic anionic excitations, useful for the construction of topological memories [33]. In addition, the possibility of varying, arbitrarily, the control parameters gives us the natural setup to study such phenomena as geometrical phases in lattice systems.

## B. Complex tunneling and topological effects

Consider the case where we employ complex tunneling couplings [34] to the optical lattice evolution. This can be performed by employing additional characteristics of the atoms, like an electric moment  $\vec{d}_e$  and an external electromagnetic field. As the external field can break time reversal symmetry, new terms of the form  $\{\sigma_j^x \sigma_{j+1}^y \sigma_{j+2}^z - \sigma_j^y \sigma_{j+1}^x \sigma_{j+2}^z\}$  appear in the effective Hamiltonian. In particular, the minimal coupling deduced from the electric dipole of the atom with the external field can be given, in general, by substituting its momentum by

$$\vec{p} \rightarrow \vec{p} + (\vec{d}_e \cdot \vec{\nabla}) \vec{A}(\vec{x}),$$

where  $\vec{A}$  is the corresponding vector potential. The new term satisfies the Gauss gauge if we demand that  $\vec{\nabla} \cdot \vec{A} = 0$ , hence it can generate a possible phase factor for the tunneling couplings.

Due to an evolution dictated by the differential form of the Aharonov-Bohm effect [35] the cyclic move of an electric moment through a gradient of a magnetic field contributes the phase

$$\phi = \int_S (\vec{d}_e \cdot \vec{\nabla}) \vec{A} \cdot d\vec{s}, \quad (4.3)$$

to the initial state, where  $S$  is the surface enclosed by the cyclic path of the electric moment. By inspection of relation (4.3) we see that a nontrivial phase can be produced if we generate an inhomogeneous magnetic field in the neighbourhood of the dipole. In particular, a non-zero gradient of the magnetic component perpendicular to the surface  $S$ , varying in the direction of the dipole, ensures a non-zero phase factor. For example, if we take  $S$  to lie on the  $x$ - $y$  plane and  $\vec{d}_e$  is perpendicular to the surface  $S$ , then a non-zero phase,  $\phi$ , is produced if there is a non-vanishing gradient of the magnetic field along the  $z$  direction. This is sketched in Figure 6(a), where the magnetic lines are plotted such that they produce the proper variation of  $B_z$  in the  $z$  direction. Alternatively, if  $\vec{d}_e$  is along the surface plane, then a non-zero phase is produced if the  $z$  component of the magnetic field has a non-vanishing gradient along the direction of  $\vec{d}_e$  as seen in Figure 6(b), where only the  $z$  component of the magnetic field has been depicted.

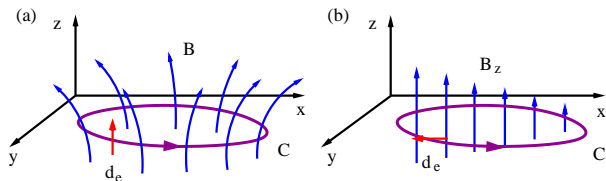


FIG. 6: The path circulation of the electric dipole in the inhomogeneous magnetic field. Figure (a) depicts magnetic field lines sufficient to produce the appropriate non-vanishing gradient of  $B_z$  along the  $z$  axis. Figure (b) depicts only  $B_z$  and how it varies along the direction of the dipole,  $\vec{d}_e$ .

We can denote by  $J = e^{i\phi}|J|$  the generation of the phase factor of the tunneling coupling between two neighbouring sites, with

$$\phi = \int_{\vec{x}_i}^{\vec{x}_{i+1}} (\vec{d}_e \cdot \vec{\nabla}) \vec{A} \cdot d\vec{x}.$$

Here  $\vec{x}_i$  and  $\vec{x}_{i+1}$  denote the positions of the lattice sites connected by the tunneling coupling  $J$ .

In order to isolate the new effects generated by the consideration of complex tunneling couplings, we restrict ourselves to purely imaginary ones, i.e.  $J_i^\sigma = \pm i|J_i^\sigma|$ . We also focus, initially, on the case where the optical lattices generate a two dimensional structure of equilateral triangles, as in Figure 7. Such a non-bipartite structure is necessary in order to manifest the breaking of the symmetry under time reversal,  $T$ , in our model, eventually producing an effective Hamiltonian that is not invariant under

complex conjugation of the tunneling couplings. Moreover, as the second order perturbation theory is manifestly  $T$  symmetric, we need to consider the third order.

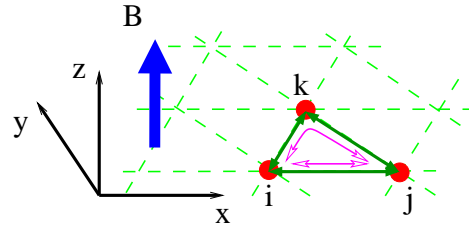


FIG. 7: The basic building block for the triangular lattice configuration. Exchange of atoms through sites  $i$  and  $j$  can happen directly or through site  $k$ , but with a phase difference, causing the generation of the chiral three-spin interaction.

In this case, the effective Hamiltonian [36], up to the second order in perturbation theory, becomes

$$H_{\text{eff}}^{(2)} = \sum_i \left[ A \mathbb{I} + B \sigma_i^z + C \sigma_i^z \sigma_{i+1}^z + D (\sigma_i^x \sigma_{i+1}^x + \sigma_i^y \sigma_{i+1}^y) \right]$$

The above couplings are given in perturbation theory by

$$A = -\frac{|J^\uparrow|^2}{U_{\uparrow\uparrow}} - \frac{|J^\downarrow|^2}{U_{\downarrow\downarrow}} - \frac{|J^\uparrow|^2 + |J^\downarrow|^2}{2U_{\uparrow\downarrow}}, \quad B = -\frac{|J^\uparrow|^2}{2U_{\uparrow\uparrow}} + \frac{|J^\downarrow|^2}{2U_{\downarrow\downarrow}},$$

$$C = -\frac{|J^\uparrow|^2}{U_{\uparrow\uparrow}} - \frac{|J^\downarrow|^2}{U_{\downarrow\downarrow}} + \frac{|J^\uparrow|^2 + |J^\downarrow|^2}{2U_{\uparrow\downarrow}}, \quad D = \frac{J^\uparrow J^\downarrow^* + J^{\uparrow*} J^\downarrow}{2U_{\uparrow\downarrow}}.$$

It is easily seen that the values of the above interactions remain unchanged compared to the case with no magnetic field. This is the case since, up to the second order perturbation theory, there are no contributions from circular paths that can experience the magnetic field. Note that it is possible to apply Raman transitions that exactly cancel the  $\sigma^z$  Zeeman term. Also, one can choose  $U_{\uparrow\downarrow} \rightarrow \infty$  (possibly by Feshbach resonances) so that  $C$  vanishes. In addition, one of the collisional couplings can be chosen to be attractive, satisfying e.g.  $U_{\uparrow\uparrow} = -U_{\downarrow\downarrow} = -U$ , so that, for  $J^{\uparrow 2} = J^{\downarrow 2}$ , the  $A$  coupling vanishes. Such attractive collisional couplings can be achieved by Feshbach resonances [37]. Stability of the system is maintained if the attractive couplings are activated adiabatically, while the atomic ensemble is in the Mott insulator regime. Since attractive couplings may eventually lead to pairing on the same lattice site, this negative  $U$  interaction can only be applied for a short period.

The third order in the perturbative expansion includes interactions between neighbouring sites via the circular path around the elementary triangle. This brings in the effect of the magnetic field, contributing a phase factor. While new interaction terms appear, the couplings  $A$ ,  $B$ ,  $C$  and  $D$  remain the same. Considering the case of



collisional and tunneling couplings, such that  $C = D = 0$ , the effective Hamiltonian becomes, up to global Zeeman terms,

$$H_{\text{eff}}^{(3)} = \sum_{\langle ijk \rangle} [E(\sigma_i^x \sigma_j^y - \sigma_i^y \sigma_j^x) + F \epsilon_{lmn} \sigma_i^l \sigma_j^m \sigma_k^n]$$

where

$$E = i \frac{J^\uparrow J^\downarrow}{2U^2} (J^\uparrow + J^\downarrow), \quad F = i \frac{J^\uparrow J^\downarrow}{2U^2} (J^\uparrow - J^\downarrow).$$

Here  $\langle ijk \rangle$  denotes nearest neighbours,  $\epsilon_{lmn}$  with  $\{l, m, n\} = \{x, y, z\}$  denotes the total antisymmetric tensor in three dimensions and summation over the indices  $l, m, n$  is implied. From the expression of the effective Hamiltonian,  $H_{\text{eff}}^{(3)}$ , it is apparent that the  $E$  and  $F$  couplings are not invariant under time reversal,  $T$ , that is, they change sign after complex conjugation. This leads to the breaking of the chiral symmetry between the two opposite circulations that atoms can take around a triangle.

By additionally taking  $J^\downarrow = -J^\uparrow = J$ , one can set all the couplings to be zero apart from  $F$  and the effective Hamiltonian reduces to

$$H_{\text{eff}}^{(3)} = F \sum_{\langle ijk \rangle} \vec{\sigma}_i \cdot \vec{\sigma}_j \times \vec{\sigma}_k, \quad (4.4)$$

with  $\vec{\sigma} = (\sigma^x, \sigma^y, \sigma^z)$  and  $F = |J|^3/U^2$ . Remarkably, with this physical proposal, the interaction term (4.4) can be isolated, especially from the Zeeman terms that are predominant in equivalent solid state implementations. This interaction term is also known in the literature as the *chirality operator* [38]. It breaks the time reversal symmetry of the system, a consequence of the externally applied field, by effectively splitting the degeneracy of the ground state into two orthogonal sectors, namely “+” and “-”, related by time reversal,  $T$ . These sectors are uniquely described by the eigenstates of  $H_{\text{eff}}^{(3)}$  at the sites of one triangle. The lowest energy sector with eigenenergy  $E_+ = -2\sqrt{3}F$  is given by

$$\begin{aligned} |\Psi_{1/2}^+\rangle &= \frac{1}{\sqrt{3}} (|\uparrow\uparrow\downarrow\rangle + \omega |\uparrow\downarrow\uparrow\rangle + \omega^2 |\downarrow\uparrow\uparrow\rangle) \\ |\Psi_{-1/2}^+\rangle &= -\frac{1}{\sqrt{3}} (|\downarrow\downarrow\uparrow\rangle + \omega |\downarrow\uparrow\downarrow\rangle + \omega^2 |\uparrow\downarrow\downarrow\rangle) \end{aligned} \quad (4.5)$$

where  $\omega^3 = 1$ . The excited sector,  $|\Psi_{\pm 1/2}^-\rangle$ , represents counter propagation with eigenvalue  $E_- = 2\sqrt{3}F$  and it is obtained from (4.5) by complex conjugation [38, 39, 40]. It has been argued that this configuration, a result of frustration due to the triangular lattice, and the disorder due to the presence of the magnetic field, leads to analogous behaviour with the fractional quantum Hall effect [38, 41] and, in particular, it can be described by the  $m = 2$  Laughlin wavefunction defined on the lattice sites. A recent example demonstrating this analogy is given in [42].

## V. ONE- AND TWO-DIMENSIONAL MODELS

It is also possible to employ the three-spin interactions that we studied in the previous sections for the construction of extended one and two dimensional systems. The two dimensional generalisation is rather straightforward as the triangular system we considered is already defined on the plane. Hence, all the interactions considered so far can be generalised for the case of a two dimensional lattice where the summation runs through all the lattice sites with each site having six neighbours.

The construction of the one dimensional model is more involved. In particular, we now consider a whole chain of triangles in the one dimensional pattern shown in Fig. 8. In principle this configuration can extend our model from the triangle to a chain. Nevertheless, a careful consideration of the two spin interactions shows that terms of the form  $\sigma_i^z \sigma_{i+2}^z$  appear in the effective Hamiltonian, due to the triangular setting (see Fig. 8). Such Hamiltonian terms involving nearest and next-to-nearest neighbour interactions are of interest in their own right [17, 18] but will not be addressed here. It is possible to introduce a longitudinal optical lattice with half of the initial wavelength, and an appropriate amplitude such that it cancels exactly those interactions generating, finally, chains with only neighbouring couplings (for more details, see VIID).

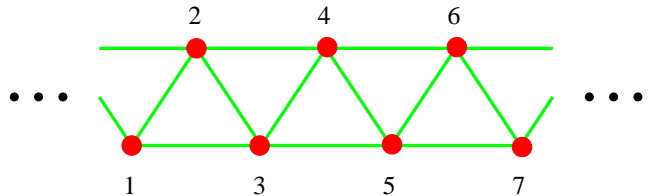


FIG. 8: The one dimensional chain constructed out of equilateral triangles. Each triangle experiences the three-spin interactions presented in the previous sections.

In a similar fashion it is possible to avoid generation of terms of the form  $\sigma_i^x \sigma_{i+2}^x + \sigma_i^y \sigma_{i+2}^y$  by deactivating the longitudinal tunneling coupling in one of the modes, e.g. the  $\uparrow$  mode, which deactivates the corresponding exchange interaction.

As we are particularly interested in three-spin interactions we would like to isolate the chain term  $\sum_i (\sigma_i^x \sigma_{i+1}^z \sigma_{i+2}^x + \sigma_i^y \sigma_{i+1}^z \sigma_{i+2}^y)$ , the  $\lambda^{(4)}$  term of Hamiltonian (3.1). This term includes, in addition, all the possible triangular permutations. To achieve that, we could deactivate the non-longitudinal tunneling for one of the two modes, e.g. the one that traps the  $\uparrow$  atoms. The interaction  $\sigma_i^z \sigma_{i+1}^z \sigma_{i+2}^z$  is homogeneous, hence it does not pose such a problem when it is extended to the one dimensional ladder. With the above procedures, we can finally obtain a chain Hamiltonian as in (3.1) where the summation runs up to the total number,  $N$ , of lattice sites.

This class of Hamiltonians gives rise to a rich variety of ground states for the spin ladder. Let us consider, as an example, the case when the tunnelling for one of the species is reduced to zero. This switches off all terms involving  $\sigma^x$  and  $\sigma^y$  in the Hamiltonian (3.1). Suppose further that we have used additional laser fields to cancel out the Zeeman term  $B\sigma^z$ . Then, the only non-zero coefficients in the Hamiltonian (3.1) are  $\lambda^{(1)}$ , the Ising interaction, and  $\lambda^{(3)}$ , the 3-spin interaction. The Hamiltonian becomes

$$H = \lambda^{(1)} \sum_i \sigma_i^z \sigma_{i+1}^z + \lambda^{(3)} \sum_i \sigma_i^z \sigma_{i+1}^z \sigma_{i+2}^z \quad (5.1)$$

Without the 3-spin interaction, the Hamiltonian describes the classical Ising model. The sign of the Ising interaction can be tuned by the relative magnitudes of the repulsive potentials  $U$ . For negative  $\lambda^{(1)}$ , the system is ferromagnetic. The up-down symmetry in the  $z$ -direction of the spin can be spontaneously broken and there are two degenerate ground states: all spins up, or all spins down. For positive  $\lambda^{(1)}$ , the ground state is the antiferromagnetic Néel state,  $|\uparrow\downarrow\uparrow\downarrow\uparrow\downarrow\cdots\rangle$  or  $|\downarrow\uparrow\downarrow\uparrow\downarrow\uparrow\cdots\rangle$ . Note that this breaks, spontaneously, the lattice translational symmetry with a spin configuration of lattice period 2.

On the other hand, if we switched off the Ising interaction with a suitable choice of  $U$ 's, the 3-spin term would give rise to different broken-symmetry ground states. For  $\lambda^{(3)} < 0$ , there are four degenerate classical ground states: a ferromagnetic state  $|\uparrow\uparrow\uparrow\cdots\rangle$  and three states with lattice period 3,  $|\uparrow\downarrow\downarrow\uparrow\downarrow\downarrow\cdots\rangle$ ,  $|\downarrow\uparrow\downarrow\uparrow\downarrow\uparrow\cdots\rangle$  and  $|\downarrow\downarrow\uparrow\downarrow\downarrow\uparrow\cdots\rangle$ . For  $\lambda^{(3)} > 0$ , the ground states are the same with  $\sigma^z$  reversed at each site. Note that the 3-spin term explicitly breaks spin-reversal symmetry, reflecting the difference in the hopping amplitudes of the two atomic species of the original system. Nevertheless, the lattice translational symmetry is spontaneously broken in the period-3 states. A small Zeeman field in the  $z$ -direction or a small antiferromagnetic Ising coupling will select out the period-3 states from the ferromagnetic state.

We can switch directly between the period-2 and period-3 ground states by tuning the interaction parameters  $\lambda^{(1)}$  and  $\lambda^{(3)}$ . The period-2 Néel state has an energy of  $-\lambda^{(1)}$  per site while the lowest-energy period-3 states have an energy of  $-\lambda^{(1)}/3 - |\lambda^{(3)}|$  per site. So, we expect a first-order phase transition along the line  $2\lambda^{(1)} = 3|\lambda^{(3)}|$ .

We can introduce quantum correlations into these models by introducing a transverse Zeeman field,  $B_x\sigma^x$ , in the Hamiltonian at each site

$$H = \sum_i \left[ \lambda^{(1)} \sigma_i^z \sigma_{i+1}^z + \lambda^{(3)} \sigma_i^z \sigma_{i+1}^z \sigma_{i+2}^z + B^x \sigma_i^x \right] \quad (5.2)$$

This transverse field gives rise to flipping between the up and down spin states (of the  $\sigma^z$  basis). The Ising chain (non-zero  $\lambda^{(1)}$  with  $\lambda^{(3)} = 0$ ) in a transverse field is a well-known model. This is discussed extensively in [17] and it can be analytically solved using the Jordan-Wigner transformation. As we increase the transverse

field  $B_x$  from zero, the magnetisation in the  $z$ -direction (ferromagnetic or antiferromagnetic according to the sign of  $\lambda^{(1)}$ ) is reduced. It vanishes at the quantum critical point  $B^x = |\lambda^{(1)}|$ . At larger values of the transverse field, the spins develop a polarisation in the  $x$ -direction. This quantum phase transition for the one-dimensional chain belongs to the same universality class as the two-dimensional classical Ising model with no transverse field.

What happens when we introduce a weak 3-spin interaction into the Ising chain with transverse field? Unfortunately, the model is not exactly solvable. As already mentioned, the 3-spin term breaks spin-reversal symmetry and so, just like a Zeeman field in the  $z$ -direction, it is a relevant perturbation in the renormalisation group sense.

Indeed, considering the opposite limit where the 3-spin interaction is strong, we know that a phase transition exists in the presence of a transverse field with the 3-spin interaction but no 2-spin Ising interaction [22, 23]. At this transition, the period-3 order parameter vanishes at  $B^x = |\lambda^{(3)}|$ . Although this transition looks analogous to the one found in an Ising chain in a transverse field, it does not belong to the same universality class as the Ising chain. It is believed that it belongs to the same universality class as the classical two-dimensional 4-state Potts model [19, 24].

This leads us to speculate about how the direct transition between period-2 and period-3 ground states is affected by the quantum fluctuations introduced by a transverse field. From the viewpoint of condensed matter physics, it will be interesting to study the critical behaviour of this model. We believe that the critical point belongs to the same universality class as the two-dimensional 3-state Potts model, borrowing arguments described in [43] for the melting of commensurate structures.

Furthermore, we note that the phases of this spin chain are similar to the quantum hard-rod system studied in [18]. That model has the additional complexity of a macroscopically large number of classically degenerate ground states at the classical transition (without transverse field). We believe that our system is easier to implement in the context of optical lattices for neutral atoms.

From the viewpoint of quantum information, it is interesting to study the degree of entanglement in this system. Indeed, we can define a reduced density matrix for  $L$  contiguous spins in a system with  $N$  spins by tracing out the other spins of the system,

$$\rho_L = \text{tr}_{N-L} |\Psi_0\rangle\langle\Psi_0|$$

where  $|\Psi_0\rangle$  is the ground state of the system [44]. A measure of how these  $L$  spins are entangled with the rest of the chain is the von Neumann entropy,

$$S_L = -\text{tr}(\rho_L \log_2 \rho_L)$$

We find that the entanglement between two halves of the system increases dramatically near the critical point (Fig.



9), similar to other studies of systems near criticality [44]. It will be interesting to investigate whether the period-2 and period-3 states can be entangled by driving the system through the transition.

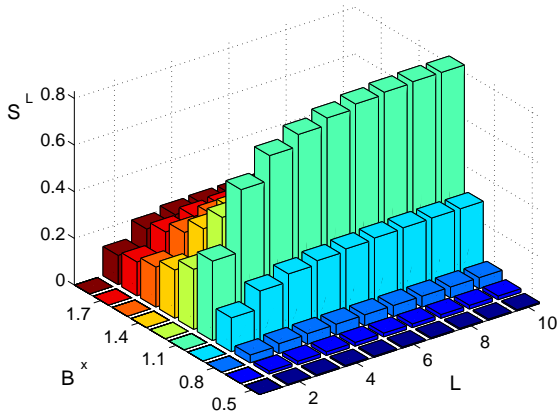


FIG. 9: The entropy  $S_L$  as a function of the length  $L$  of the reduced density matrix and the transverse magnetic field  $B_x$  for  $\lambda^{(3)} = 1$ . The critical behaviour is indicated at the point  $B_x \approx 1$ .

## VI. LOCALISABLE ENTANGLEMENT AND CLUSTER HAMILTONIAN

In the past, Hamiltonians describing three-spin interactions have been of limited interest [19, 20] as they were difficult to implement and control experimentally. The previous results demonstrate that Hamiltonians with three-spin interactions can be implemented and parameters controlled across a wide intervals. One may suspect that ground states of three-spin interaction Hamiltonians exhibit unique properties as compared to ground states generated merely by two-spin interactions. This motivates the study of the properties of the ground state of a particular three-spin Hamiltonian for different parametric regimes. Possible phase transitions induced by varying these parameters are explored employing two possible signatures of critical behaviour that are quite different in nature. In particular, new critical phenomena in three-spin Hamiltonians that cannot be detected on the level of classical correlations will be demonstrated.

(i) A traditional approach to criticality of the ground state studies two-point correlation functions between spins 1 and  $L$ , given by  $C_{1L}^{\alpha\beta} \equiv \langle \sigma_1^\alpha \sigma_L^\beta \rangle - \langle \sigma_1^\alpha \rangle \langle \sigma_L^\beta \rangle$ , for varying  $L$ , where  $\alpha, \beta = x, y, z$ . These two-point correlations may exhibit two types of generic behaviour, namely (a) exponential decay in  $L$ , i.e. the correlation length  $\xi$ , defined as

$$\xi^{-1} \equiv \lim_{L \rightarrow \infty} \frac{1}{L} \log C_{1L}^{\alpha\beta}, \quad (6.1)$$

is finite or, (b), power-law decay in  $L$ , i.e.  $C_{1L}^{\alpha\beta} \sim L^{-q}$  for some  $q$ , which implies an infinite correlation length  $\xi$  indicating a critical point in the system [17].

(ii) While the two-point correlation functions  $C_{1L}^{\alpha\beta}$  are a possible indicator for critical behaviour, they provide an incomplete view of the quantum correlations between spins 1 and  $L$ . Indeed, they ignore correlations through all the other spins, by tracing them out. Considering, for example, the GHZ state,  $|GHZ\rangle = (|000\rangle + |111\rangle)/\sqrt{2}$ , already shows that this loses important information. Tracing out particle 2 leaves particles 1 and 3 in an unentangled state. However, measuring the second particle in the  $\sigma_x$ -eigenbasis leaves particles 1 and 3 in a maximally entangled state. Therefore one may define the localisable entanglement  $E_{1L}^{(loc)}$  between spins 1 and  $L$  as the largest average entanglement that can be obtained by performing optimised local measurements on all the other spins [45]. In analogy to Eqn. (6.1) one can define the entanglement length,  $\xi_E$ , by

$$\xi_E^{-1} \equiv \lim_{L \rightarrow \infty} \frac{1}{L} \log E_{1L}^{(loc)}. \quad (6.2)$$

It is now an interesting question whether criticality according to one of these indicators implies criticality according to the other. The localisable entanglement length is always larger than, or equal to, the two-point correlation length and indeed, it has been shown that there are cases where criticality behaviour can be revealed only by the diverging localisable entanglement length while the classical correlation length remains finite [16, 46]. Such behaviour is also expected to appear when we consider particular three-spin interaction Hamiltonians. To see this consider the Hamiltonian

$$H = \sum_i (\sigma_{i-1}^x \sigma_i^z \sigma_{i+1}^x + B \sigma_i^z), \quad (6.3)$$

where we assume periodic boundary conditions. The fact that  $\sigma_{i-1}^x \sigma_i^z \sigma_{i+1}^x$  commute for different  $i$  and employing raising operator  $L_k^\dagger = \sigma_k^x - i \sigma_{k-1}^y \sigma_k^y \sigma_{k+1}^x$  allows to determine the entire spectrum of  $H$  for  $B = 0$  quite easily. The unique ground state of  $H$  for  $B = 0$  is the well-known cluster state [47, 48], which has previously been studied as a resource in the context of quantum computation. It possesses a finite energy gap of  $\Delta E = 2$  above its ground state [49]. For finite  $B$  the energy eigenvalues of the system can still be found using the Jordan-Wigner transformation and a lengthy, but straightforward, calculation shows that the energy gap persists for  $|B| \neq 1$ . The exact solution also shows that the system has critical points for  $|B| = 1$  at which the two-point correlation length and the entanglement length diverge. For any other value of  $B$  and in particular for  $B = 0$ , the system does not exhibit a diverging two-point correlation length as is expected from the finite energy gap above the ground state. Indeed, correlation functions such as

$$C_{ab}^{zz} = \psi_{ab}^2 - \chi_{ab}^2, \quad (6.4)$$

with

$$\psi_{ab} \equiv \frac{1}{4\pi} \int_{-2\pi}^{2\pi} \frac{\sin r}{\sqrt{B^2 + 1 + 2B \cos r}} \sin \frac{(b-a)r}{2} dr, \quad (6.5)$$

and

$$\chi_{ab} \equiv \frac{1}{4\pi} \int_{-2\pi}^{2\pi} \frac{B + \cos r}{\sqrt{B^2 + 1 + 2B \cos r}} \cos \frac{(b-a)r}{2} dr. \quad (6.6)$$

can be computed and the corresponding correlation length can be determined analytically using standard techniques (see e.g. Fig. (10)) [50]. The two-point correlation functions, such as Eqn. (6.4), exhibit a power-law decay at the critical points  $|B| = 1$  while they decay exponentially for all other values of  $B$  in contrast to the anisotropic  $XY$ -model whose  $C_{1L}^{xx}$  correlation function tends to a finite constant in the limit of  $L \rightarrow \infty$  for  $|B| < 1$  [50]. This discrepancy is due to the finite energy gap the model in Eqn. (6.3) exhibits above a non-degenerate ground state in the interval  $|B| < 1$ .

When we study three-spin interactions it is natural to consider the behaviour of higher-order correlations. For the ground state with magnetic field  $B = 0$ , all three-point correlation except, obviously,  $\langle \sigma_{i-1}^x \sigma_i^z \sigma_{i+1}^x \rangle$  vanish. Indeed, if we consider  $n > 4$  neighbouring sites and choose for each of these randomly one of the operators  $\sigma_x, \sigma_y, \sigma_z$  or  $\mathbb{I}$  then the probability that the resulting correlation will be non-vanishing is given by  $p = 2^{-(2+n)}$ . For  $|B| > 0$ , however, far more correlations are non-vanishing and the rate of non-vanishing correlations scales approximately as  $0.858^n$ . This marked difference, which distinguishes  $B = 0$ , is due to the higher symmetry that the Hamiltonian exhibits at that point.

In the following we shall consider the localisable entanglement and the corresponding length as described in (ii). Compared to the two-point correlations, the computation of the localisable entanglement is considerably more involved due to the optimisation process. Nevertheless, it is easy to show that the entanglement length diverges for  $B = 0$ . In that case the ground state of the Hamiltonian (6.3) is a cluster state with the property that any two spins can be made deterministically maximally entangled by measuring the  $\sigma_z$  operator on each spin in between the target spins, while measuring the  $\sigma_x$  operator on the remaining spins. Indeed, this property underlies its importance for quantum computation as it allows us to propagate a quantum computation through the lattice via local measurements [48].

For finite values of  $B$  it is difficult to obtain the exact value of the localisable entanglement. Nevertheless, to establish a diverging entanglement length it is sufficient to provide lower bounds that can be obtained by prescribing specific measurement schemes. Indeed, for the ground state of (6.3) in the interval  $|B| < 1$ , consider two spins 1 and  $L = 2k + 1$  where  $k \in \mathbf{N}$ . Measure the  $\sigma_x$  operator on spin 2 and on all remaining spins, other than 1 and  $L$ , measure the  $\sigma_z$  operator. By knowing the analytic form of the ground state one can ob-

tain the average entanglement over all possible measurement outcomes in terms of the concurrence, that tends to  $E_\infty = (1 - |B|^2)^{1/4}$  for  $k \rightarrow \infty$ . This demonstrates that the localisable entanglement length is infinite in the full interval  $|B| < 1$ . This surprising critical behaviour for the whole interval  $|B| < 1$  is *not* evident from simple two-point or  $n$ -point correlation function which exhibit finite correlation lengths. For  $|B| > 1$  however, numerical results, employing a simulated annealing technique to find the optimal measurement for a chain of 16 spins, show that the localisable entanglement exhibits a finite length scale.

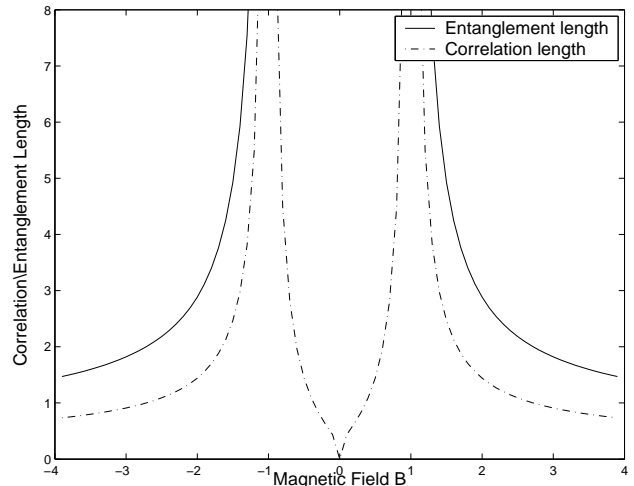


FIG. 10: Both, the two-point correlation length for  $C_{1L}^{zz}$  (dashed line) and the localisable entanglement length (solid line) are shown for various magnetic field for chain of length 16. Note that the localisable entanglement length diverges in the whole interval  $|B| < 1$  while the two-point correlation length is finite in this interval.

From a practical point of view it is of interest to see how resilient these predicted features are with respect to noise. To this end, note that in Fig. (10) both the two-point correlation length and localisable entanglement length are drawn versus the magnetic field. In the interval  $|B| < 1$  the entanglement length diverges while the correlation length remains finite. For finite temperatures the localisable entanglement becomes finite everywhere but, for temperatures that are much smaller than the gap above the ground state, it remains considerably larger than the classical correlation length. This demonstrates the resilience of this phenomenon against thermal perturbations.

The preceding analysis of our three-spin interaction Hamiltonian (6.3) has indicated a marked qualitative discrepancy between the localisable entanglement length and the two-point correlation length with regard to variations in the magnetic field strength parameter,  $B$ : across the interval between the two critical points,  $|B| < 1$ ,

the former quantity diverges while the latter remains finite. We surmised that knowledge of simple two-point correlation functions (such as  $C_{ab}^{zz}$ ) alone is insufficient in order to arrive at a complete characterisation of criticality. Nevertheless, the question remains whether the aforementioned discrepancy could not be reconciled by some non-trivial *combination* (motivated by quantum information theory) of two-point correlation functions. A natural and easily computable candidate for such a quantity is the logarithmic negativity [51] (for basic ideas of the theory of entanglement measures see, for example, [52]), which serves as a practical tool in the endeavour to quantify multipartite entanglement. The logarithmic negativity of a quantum state  $\rho$  is defined as

$$E_N \equiv \log_2 \text{tr} |\rho^\Gamma|, \quad (6.7)$$

where  $\rho^\Gamma$  denotes the partial transpose of the density operator and  $\text{tr}|\cdot|$  refers to the trace-norm, i.e. the sum of the singular values of the operator.

We are interested in the entanglement, as measured by the logarithmic negativity, between two spin- $\frac{1}{2}$  particles residing at sites  $i$  and  $j$  on the chain modelled by Hamiltonian (6.3). The composite state for the pair of spins is described by the two-site reduced density matrix,  $\rho_{ij}$ , which is formally obtained from the total density matrix (describing the ground state of the whole chain) by tracing out all the spin degrees of freedom apart from the two spins under consideration.

In practice, however, the easiest procedure is to expand the general two-site density matrix in the trace-orthogonal basis formed by the tensor products of the Pauli spin operators at either site as

$$\rho_{ij} = \frac{1}{4} \sum_{\alpha, \beta=0}^3 \langle \sigma_i^\alpha \sigma_j^\beta \rangle \sigma_i^\alpha \otimes \sigma_j^\beta,$$

where the expansion coefficients are expectation values with respect to the ground state of the Hamiltonian. It is useful to represent this operator expansion in the standard two-qubit basis,  $\{|\uparrow\uparrow\rangle, |\uparrow\downarrow\rangle, |\downarrow\uparrow\rangle, |\downarrow\downarrow\rangle\}$ , where  $|\uparrow\rangle$  and  $|\downarrow\rangle$  represent the eigenstates of  $\sigma^z$  with eigenvalues  $+1$  and  $-1$ , respectively. In that basis,

$$\rho_{ij} = \sum_{\alpha, \beta=0}^3 \langle s_i^\alpha s_j^\beta \rangle s_i^\alpha \otimes s_j^\beta,$$

with  $s^0 \equiv |\uparrow\rangle\langle\uparrow| = \frac{1}{2}(\mathbb{I} + \sigma^z)$ ,  $s^1 \equiv |\downarrow\rangle\langle\downarrow| = \frac{1}{2}(\mathbb{I} - \sigma^z)$ ,  $s^2 \equiv |\uparrow\rangle\langle\downarrow| = \sigma^+$ ,  $s^3 \equiv |\downarrow\rangle\langle\uparrow| = \sigma^-$ .

A priori, the construction of  $\rho_{ij}$  then requires knowledge of sixteen expansion coefficients,  $\langle s_i^\alpha s_j^\beta \rangle$ . Owing to symmetry properties of the Hamiltonian, however, these are not all independent. For example, the Hamiltonian possesses the global phase-flip symmetry  $[H, U] = 0$ , where  $U = \otimes_{j=1}^N \sigma_j^z$ . This symmetry then carries over directly to the two-site reduced density matrix obtained from the global ground state in the form  $[\rho_{ij}, \sigma_i^z \sigma_j^z] = 0$ ,

forcing half of its matrix elements to vanish. Furthermore, translational invariance of the Hamiltonian dictates that  $\rho_{\uparrow\downarrow, \uparrow\downarrow} = \rho_{\downarrow\uparrow, \downarrow\uparrow}$  (here and henceforth we drop the indices  $i$  and  $j$ ). Finally, the reduced density matrix must be a real, symmetric matrix with unity trace.

Having taken the Hamiltonian's symmetries into consideration, we find that the reduced density matrix possesses three distinct diagonal elements,

$$\begin{aligned} \rho_1 &\equiv \rho_{\uparrow\uparrow, \uparrow\uparrow} = (1 + 2\langle\sigma^z\rangle + \langle\sigma_i^z \sigma_j^z\rangle)/4, \\ \rho_2 &\equiv \rho_{\uparrow\downarrow, \uparrow\downarrow} = (1 - \langle\sigma_i^z \sigma_j^z\rangle)/4, \\ \rho_3 &\equiv \rho_{\downarrow\downarrow, \downarrow\downarrow} = (1 - 2\langle\sigma^z\rangle + \langle\sigma_i^z \sigma_j^z\rangle)/4, \end{aligned}$$

and two distinct non-zero off-diagonal elements,

$$\rho_+ = \rho_{\uparrow\uparrow, \downarrow\downarrow} = \langle\sigma_i^+ \sigma_j^+\rangle, \quad \rho_- = \rho_{\downarrow\downarrow, \uparrow\uparrow} = \langle\sigma_i^+ \sigma_j^-\rangle.$$

The reduced density matrix is therefore uniquely determined by the set of four expectation values,  $\{\langle\sigma^z\rangle, \langle\sigma_i^z \sigma_j^z\rangle, \langle\sigma_i^+ \sigma_j^+\rangle, \langle\sigma_i^+ \sigma_j^-\rangle\}$ .

Since the reduced density matrix between nearest neighbours does not exhibit entanglement for any value of the magnetic field  $B$  we will now consider the reduced density matrix with respect to a ‘‘bridge pair’’ of spins (any pair of spins sandwiching a third). Given the translational invariance of the Hamiltonian, we may restrict our study to sites 1 and 3, without loss of generality. The partial transpose of the reduced density matrix with respect to either subsystem differs from the original matrix only through an interchange of  $\rho_+$  and  $\rho_-$  (along with  $\{i, j\}$  and  $\{1, 3\}$ ). Its four eigenvalues are given by

$$\lambda_{1,2} = \frac{(\rho_1 + \rho_3) \pm \sqrt{(\rho_1 + \rho_3)^2 - 4(\rho_1 \rho_3 - \rho_-^2)}}{2}$$

and

$$\lambda_{3,4} = \rho_2 \pm \rho_+.$$

In order to quantify the entanglement within our bridge pair, all that remains is to compute the set of four simple expectation values that constitute the raw ingredients for the pair's reduced density matrix. We are especially interested in the thermodynamic limit, where  $N \rightarrow \infty$  and we are no longer dealing with complicated sums, but with manageable integrals. In fact, all four expectation values are simple combinations of the two integrals, Eqs. (6.5) and (6.6), defined earlier:

$$\begin{aligned} \langle\sigma^z\rangle &= -\chi_{00}, \quad \langle\sigma_1^z \sigma_3^z\rangle = \chi_{00}^2 + \psi_{13}^2 - \chi_{13}^2, \\ \langle\sigma_1^+ \sigma_3^+\rangle &= \frac{1}{2}\psi_{13}\langle\sigma^z\rangle, \quad \langle\sigma_1^+ \sigma_3^-\rangle = \frac{1}{2}\chi_{13}\langle\sigma^z\rangle. \end{aligned}$$

For a few special values of  $B$ , these integrals, and the associated logarithmic negativity, can be computed precisely with ease. The results are summarised in the table below.

	magnetic field strength				
	$-\infty$	$-1$	$0$	$1$	$\infty$
$\psi_{13}$	0	$\frac{4}{3\pi}$	$\frac{1}{2}$	$\frac{4}{3\pi}$	0
$\chi_{13}$	0	$\frac{2}{3\pi}$	$\frac{1}{2}$	$\frac{2}{3\pi}$	0
$\langle \sigma^z \rangle$	1	$\frac{2}{\pi}$	0	$-\frac{2}{\pi}$	-1
$\langle \sigma_1^z \sigma_3^z \rangle$	1	$\frac{16}{3\pi^2}$	0	$\frac{16}{3\pi^2}$	1
$\langle \sigma_1^+ \sigma_3^+ \rangle$	0	$\frac{4}{3\pi^2}$	0	$-\frac{4}{3\pi^2}$	0
$\langle \sigma_1^+ \sigma_3^- \rangle$	0	$\frac{2}{3\pi^2}$	0	$-\frac{2}{3\pi^2}$	0
$\sum_i  \lambda_i $	1	$\frac{1}{2} + \frac{16}{3\pi^2}$	1	$\frac{1}{2} + \frac{16}{3\pi^2}$	1
	0	0.05711...	0	0.05711...	0
	<b>logarithmic negativity</b>				

For general  $B$ , the integrals are most easily computed numerically. A plot of the logarithmic negativity versus the magnetic field strength is shown in Fig. (11).

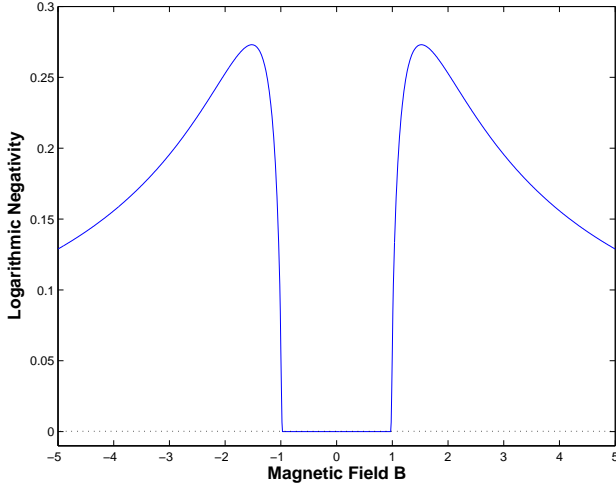


FIG. 11: The logarithmic negativity is shown as a function of the magnetic field strength parameter  $B$  in the thermodynamic limit  $N \rightarrow \infty$ .

From among the features discernible in Fig. (11), we are primarily interested in the interval enclosed by the two critical points,  $|B| \leq 1$ , where the logarithmic negativity appears to vanish identically. That characteristic would be directly analogous to the diverging localisable entanglement length encountered in Fig. (10). Close inspection reveals, however, that the logarithmic negativity grows positive even before reaching the critical points,  $B_c = \pm 1$ . This phenomenon already suggested itself as a result of our analytical computation of the logarithmic negativity (c.f. the provided table), and is most discernibly manifest in Fig. (12), which provides a close-up of the area immediately surrounding  $B_c = 1$ .

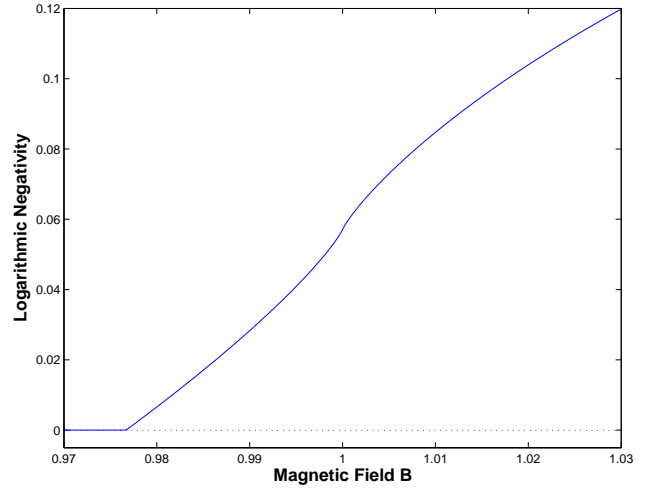


FIG. 12: Here, Fig. (11) is magnified in a small interval centred around the point  $B_c = 1$ . The logarithmic negativity is clearly seen to take on positive values before reaching  $B_c = 1$ .

Note that we may bypass many steps involved in the computation of the logarithmic negativity if we are not concerned with its precise value across the whole range of  $B$ , but are merely interested in establishing the region where it vanishes. For that purpose, it suffices to check that the eigenvalues corresponding to the reduced density matrix are all positive semi-definite. That requirement is succinctly contained in the pair of inequalities  $\rho_1 \rho_3 \geq \rho_2^2$  and  $\rho_2 \geq |\rho_+|$ . In the event, it turns out that the latter inequality is all that is needed here, because the former condition is already satisfied for all values of the parameter  $B$ .

A note of caution with regard to predictions on the basis of spin chains with finite length: such finite chains are prone to uncharacteristic behaviour, particularly in the vicinity of a quantum phase transition. As an example, let us consider how the logarithmic negativity with respect to a bridge pair of spins varies as a function of the spin chain's length. Such a scenario is depicted in Fig. (13), with the parameter  $B$  chosen to lie within the range of values where the logarithmic negativity is non-vanishing in the thermodynamic limit (see Fig. (12));  $B = 0.9875$  to be precise.

Fig. (13) points to a remarkable finite-size effect: the diagram is composed of three separate curves, the middle one representing chains of odd lengths and the other two together making up the even lengths. Furthermore, one of the curves (representing lengths where  $N + 2$  is a multiple of four) stays identically zero to start off with, until it abruptly rises to converge with the other two curves. The diagram sees the logarithmic negativity converge to a value around 0.0226, which is in complete agreement with the plot of Fig. (12) at the same value of  $B$ . For all intents and purposes,  $N = 700$  can therefore already

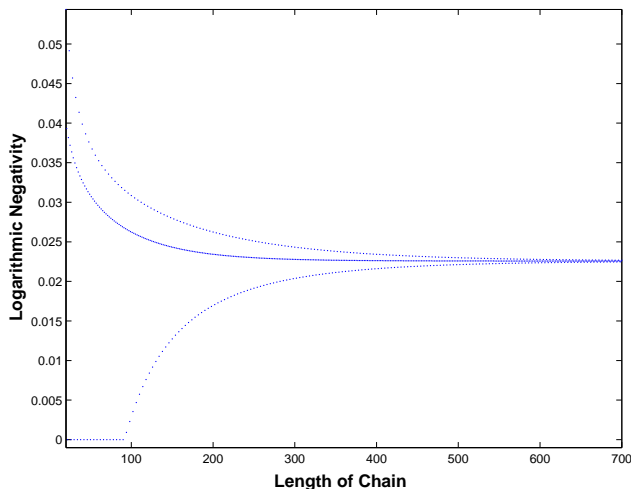


FIG. 13: The logarithmic negativity with respect to a bridge pair of spins is shown as a function of the spin chain’s length, with the magnetic field strength parameter  $B$  set to 0.9875. The graph indicates a marked finite-size effect, which vanishes in the thermodynamic limit. The middle curve represents chains with an odd number of spins, while the other two curves make up the even chain lengths. All three curves converge to a common value as the chain length increases.

be regarded as representing an infinitely long chain for this particular value of  $B$ . Predictably, as the coupling parameter is steadily increased to  $B_c = 1$ , the three curves converge to an increasingly higher value (reaching 0.5711... at  $B_c = 1$ ), and the rate of convergence increases simultaneously. However, when we increase the coupling parameter further still, another surprising finite-size effect occurs. Precisely where the coupling parameter surpasses the critical point  $B_c = 1$ , the bottom curve of Fig. (13) (now strictly positive for all  $N$ ) experiences a dramatic jump and approaches the convergence with the other two curves *from above*. The size of this phenomenon diminishes with increasing chain length and vanishes all together for infinitely long chains, as is evident from Fig. (12). So it would actually appear that the much sought-after critical behaviour in the entanglement measure turns out to be a finite-size effect that vanishes in the thermodynamic limit!

In summary, we embarked upon the preceding investigation in quest of a simple order parameter that would allow us to predict the occurrence of an infinite localisable entanglement length. A combination of two-point correlation functions motivated by quantum information science, the logarithmic negativity was deemed to be a suitable candidate for such an order parameter, but our findings have since led us to conclude that this measure cannot, in general, predict the behaviour of the localisable entanglement length. This further substantiates the belief that the localisable entanglement length in translation invariant systems is a novel concept that transcends mere two-point correlation functions.

## VII. QUANTUM COMPUTATION

We have already seen how, in an optical lattice, for a single triangle, one can manipulate, by varying suitably the tunneling and/or the collisional couplings, the interaction terms of the form  $\sigma_j^x \sigma_{j+1}^x + \sigma_j^y \sigma_{j+1}^y$ ,  $\sigma_j^z \sigma_{j+1}^z$ ,  $\sigma_j^z \sigma_{j+1}^z \sigma_{j+2}^z$  and  $\sigma_j^z (\sigma_{j+1}^x \sigma_{j+2}^x + \sigma_{j+1}^y \sigma_{j+2}^y)$ . These interactions, up to common single qubit rotations, are equivalent to quantum gates where the states  $|\uparrow\rangle$  and  $|\downarrow\rangle$  represent the logical states  $|0\rangle$  and  $|1\rangle$  of the computation. From the above interactions, one can obtain SWAP, controlled-Phase ( $CP$ ), controlled-controlled-Phase ( $C^2P$ ) and controlled-SWAP (cSWAP) respectively. In the following subsection we shall see how this is achieved. In particular, the  $CP$  and  $C^2P$  gates are produced by manipulating *one* of the two optical lattice modes while the other remains with a high amplitude, corresponding to zero tunneling. The exchange interaction (SWAP) is produced by lowering the barriers that trap *both* the  $|0\rangle$  and  $|1\rangle$  states as seen in (3.1).

We shall then proceed to show how these gates can be combined to perform quantum computation on one- or two-dimensional structures, such as those described in section V, without the need for targeting specific lattice sites i.e. we will only control fields that are applied globally, to the whole system [6, 53, 54, 55, 56].

There are two key ideas in targeting operations to specific qubits by global addressing. Firstly, we employ a specific qubit as a pointer and, secondly, we consider the effect of double wavelength fields for addressing alternate triangles. We expand on both of these ideas in subsequent subsections.

### A. Quantum Gates from Interactions

In order to create quantum gates from the interactions that we have, let us define

$$\Lambda_i = \int_0^T \lambda^{(i)} dt$$

where  $\lambda^{(0)} = B$  (3.1). This encapsulates the variation with time of the coupling strengths as various optical lattices are applied. The results should always be taken modulo  $2\pi$ , due to the exponentiation procedure. The time,  $T$ , will be the same for each  $\Lambda_i$  for a given gate but can, naturally, be different for the different gates that we wish to create.

Gate	$\Lambda_0$	$\Lambda_1$	$\Lambda_2$	$\Lambda_3$	$\Lambda_4$
$CP$	$-\frac{\pi}{4}$	$\frac{\pi}{4}$	0	0	0
$C^2P$	$\frac{\pi}{8}$	$-\frac{\pi}{8}$	0	$\frac{\pi}{8}$	0
SWAP	0	0	$\frac{\pi}{2}$	0	0
cSWAP	0	0	$\frac{\pi}{4}$	0	$-\frac{\pi}{4}$

Indeed, the above table shows how to create the quantum gates from the different terms of the Hamiltonian

(3.1). As presented, both SWAP and cSWAP generate an extra phase gate. This effect can also be negated, but has been left out for simplicity.

## B. Organisation of the Computer

We start with a one dimensional ladder of triangles, as shown in Figure 8 and again in Figure 14(a), although this can easily be extended to two dimensions. We label one horizontal line as the register array, and the other as the auxiliary array. The register array will contain the qubits that we perform the computation on while the auxiliary array will facilitate the transport of the pointer. The whole system is initialised such that every qubit is in the  $|0\rangle$  state. We require a pointer to help us localise operations. This is achieved by retaining single qubit control over a single lattice site, so we can flip that qubit into the  $|1\rangle$  state.

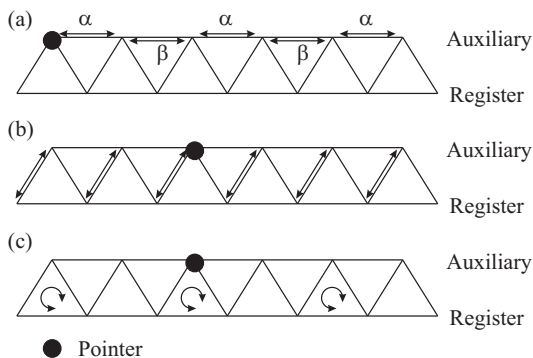


FIG. 14: (a) The one dimensional chain of triangles divided into a row of auxiliary and register qubits. All are initialised as a  $|0\rangle$  apart from the pointer, which is in the state  $|1\rangle$ . The interactions required to transport the pointer are also indicated.  $\alpha$  and  $\beta$  exchange interactions can be controlled separately. (b) Interactions required to create the  $CP$  gate, yielding  $\sigma_z$  on a single qubit. (c) Interactions required to create  $C^2P$  gate on alternate triangles.

The basic idea is that if we can create a  $CP$  gate between lattice sites along the lines shown in Figure 14(b), then this acts as a  $\sigma_z$  gate being applied only to the qubit adjacent to the pointer. If we can also create a  $C^2P$  gate on alternate triangles, for example around the triangles shown in Figure 14(c), then this is just like creating a  $CP$  gate between the two qubits on the same triangle as the pointer without affecting at all the rest of the register qubits. These actions are the main building blocks for performing universal quantum computation with our setup.

## C. Moving the pointer and qubits

We have specified how certain gates can be created when the pointer is next to a specific qubit, or when the pointer and two specific qubits are all located at the vertices of the same triangle. However, we need to know how to move the pointer and the qubits so that they can interact as we want them to. To achieve this, we use the SWAP operation applied to alternate qubits.

Moving the pointer is a relatively simple matter if we have a system of SWAPs available. We just switch between the two SWAP-ing modes along the top of the chain, denoted by  $\alpha$  and  $\beta$  in Figure 14(a). This allows us to move the pointer to any arbitrary position on the chain. Exactly the same idea can be applied to the register qubits, provided they are separated by an even number of qubits. If they are separated by an odd number of qubits, then applying SWAPs just causes the two qubits to move together, with constant separation. To avoid this, we have to use the pointer to apply a controlled-SWAP to one of the qubits so that it becomes separated from the other qubit by an even number. We have already shown one method for generating this cSWAP, using the natural Hamiltonian of the system. It can also be built by standard gates, which we shall see how to construct in the following.

## D. Superlattices

In order to activate certain Hamiltonian terms on alternate triangles, we need to employ the idea of superlattices. These are obtained by superposing on the trapping potentials standing wave fields with a different period. The idea is illustrated in Figure 15. To generate these superlattices, it is not necessary to have a large set of lasers with different wavelengths. Instead of setting them up in direct opposition, it is possible to create standing waves with varying periodicity by introducing an angle between them [57, 58]. This angle determines the period of the standing wave,  $d_i$  given by

$$d_i = \frac{\lambda}{2 \sin(\theta_i/2)}$$

The required manipulation of potentials for triangular lattices demands the activation of tunnelings along certain sites, while it should be prohibited along other ones. For example, to create the alternating SWAP that we require for moving the pointer (Figure 14(a)), we need to ensure that we don't activate couplings between the register and the auxiliary arrays. We also only want to activate couplings on every other horizontal line. Hence, we specify that we require a potential of the form

$$V_{\text{off}} = \cos(kx) \sin\left(\frac{ky}{\sqrt{3}}\right) \sin\left(\frac{ky}{\sqrt{3}} - kx\right) \sin\left(\frac{ky}{\sqrt{3}} + kx\right),$$



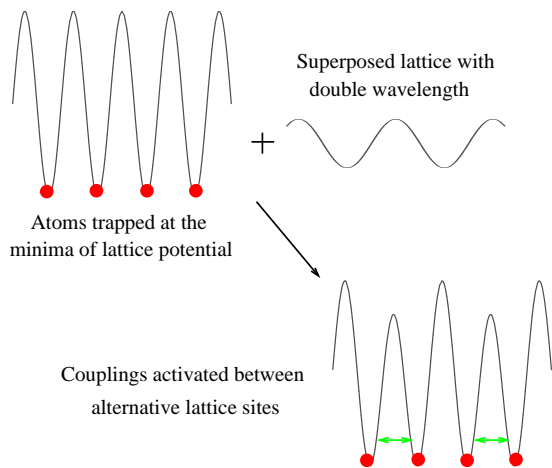


FIG. 15: Illustration of how a laser with double the wavelength of the trapping potential can activate alternate couplings, as required for the SWAP procedure (for example).

taking the origin to be located on one of the register qubit lattice sites. This can be expanded as a series of sine functions, each of which can be created by a pair of lasers resulting in the desired pattern, given in Fig. 16. The determination of orientation and angle for the laser pairs is demonstrated in [6] using the simpler example of a square lattice.

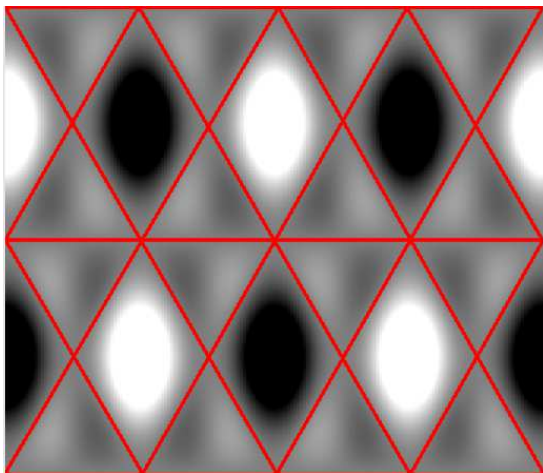


FIG. 16: The potential offset that activates tunneling transitions between alternate lattice sites. The darker areas indicate lowering of the potential barrier, while the lighter areas indicate its increase. The straight lines indicate constant potential. The qubits are located at the vertices of these lines.

### E. Universal Quantum Computation

So far, we have shown how to create a certain set of interactions as we require them -  $CP$ ,  $C^2P$ , SWAP and

$c$ SWAP. If we can also apply single qubit rotations to alternate lines of the lattice, then we can apply sequences such as  $U$ ,  $CP$  and  $U^\dagger$ , which have no effect if the auxiliary qubit is in the  $|0\rangle$  state because  $U$  and  $U^\dagger$  cancel, but applies  $U\sigma_z U^\dagger$  to the qubit targeted by the pointer. We are then able to create, by this process, any single qubit rotation on a given qubit. Together with the  $CP$  gate (or  $\sqrt{\text{SWAP}}$  gate, which is generated using the same procedure as for the  $c$ SWAP, for only half the time), it constitutes a set of universal gates for quantum computation.

The single qubit rotations, created by Raman transitions on alternate rows of the lattice, can, again, be generated by a standing wave of double the period, so that the 0's of potential are localised on the rows that we don't want to experience the rotation. The lasers that create this standing wave need to be of a different wavelength to all the others to avoid undesired transitions taking place.

### F. Error Prevention and Correction

Errors are the bane of any implementation of quantum computation, and there is much research on minimising their effects with better quality apparatus and by using decoherence free subspaces [59, 60]. It is known that once we are able to perform operations with an error that is below a certain threshold (assuming any errors leave the qubits within the computational subspace), it is possible to perform arbitrarily accurate quantum computation through the process of concatenation of quantum error correcting codes [61], leading to fault tolerance [62]. It has recently been shown that the same can be done for globally controlled systems such as the one presented here [55, 63].

The first thing to note is that the auxiliary array always remains in a classical state. This instantly protects it against  $\sigma_z$  errors, since classical states are eigenstates of  $\sigma_z$ . We can also protect against  $\sigma_x$  errors by constantly measuring the state of the qubits via the Quantum Zeno effect. Note that, if we measure the auxiliary array in the  $|1\rangle$  state, we risk losing the pointer. We choose, instead, to measure only every other qubit on the auxiliary array, not including the pointer. This at least provides an indication of whether or not there has been an error on the pointer.

We can also employ this idea to provide measurement at the end of the computation. We achieve this by performing a  $c$ SWAP around a triangle so that we move a qubit from the register array onto the auxiliary array, next to the pointer. We are then able to perform the measurement.

Finally, the qubits on the register array can be encoded into a quantum error correcting code. Sufficient parallelism can be generated within the array to allow for error correction on every block of encoded qubits (see [6, 55] for more details). Instead of correcting the errors by making a measurement and then performing the

relevant correction, these steps are performed by an algorithm that uses controlled-NOT gates to correct for the errors, as determined by the error syndrome stored on ancilla qubits. The problem with this method is that to perform the syndrome extraction (placing on auxiliary qubits information about the errors), the ancilla qubits must be in a well-known state ( $|0\rangle$ ). After the error correcting phase, these qubits are left in an unknown state. Hence, it is necessary to either reset the state of the qubits, or have a large supply of fresh qubits. In the optical lattice set-up, this second option is quite sensible. We have so far restricted computation to a single two-dimensional plane. However, in a three dimensional lattice there are many of these planes, all of which contain qubits in the  $|0\rangle$  state. If we perform our computation on a single plane, then this plane can be moved through all the other planes by a series of SWAPs between alternate planes. We can therefore access this large supply of fresh qubits for the purposes to error correction without the need to perform measurements during the computation, thus simplifying the experimental implementation.

### VIII. CONCLUSIONS

In this paper we presented, initially, a variety of different spin interactions that can be generated by a system of ultra-cold atoms superposed by optical lattices and initiated in the Mott insulator phase. In particular, we have been interested in the simulation and study of various three-spin interactions conveniently obtained in a lattice with equilateral triangular structure. The possibility to externally control most of the parameters of the effective Hamiltonians at will renders our model as a unique lab-

oratory to study the relationship among exotic systems such as chiral spin systems, fractional quantum Hall systems or systems that exhibit high- $T_c$  superconductivity [26, 38]. Furthermore, unique properties related with the critical behaviour of the chain with three-spin interactions has been analysed (see also [16]) where the two-point correlations, used traditionally to describe the criticality of a chain, seem to fail to identify long quantum correlations, suitably expressed by a variety of entanglement measures [45]. In particular, analysing the logarithmic negativity, indicates a possible connection between the localisable entanglement length on the one hand and entanglement properties of closely spaced spins on the other. In addition, suitable applications have been presented within the realm of quantum computation [6, 27] where three-qubit gates can be straightforwardly generated from the three-spin interactions.

In conclusion the three-spin interactions generated in an optical lattice offer a rich variety of applications in quantum information technology as well as in solid state physics, worth pursuing further theoretically and experimentally.

### Acknowledgments

J. P. would like to thank Christian D’Cruz for useful conversations. This work was supported by a Royal Society University Research Fellowship, a Royal Society Leverhulme Trust Senior Research Fellowship, the EPSRC QIP-IRC, the EU Thematic Network QUPRODIS and by the Spanish grant MECD AP2001-1676. E.R. thanks the QI group at DAMTP for their hospitality, where part of this work was done.

- 
- [1] A. Kastberg, W. D. Phillips, S. L. Rolston, R. J. C. Spreeuw, and P. S. Jessen, *Phys. Rev. Lett.* **74**, 1542 (1995); G. Raithel, W. D. Phillips, and S. L. Rolston, *Phys. Rev. Lett.* **81**, 3615 (1998).
  - [2] M. Greiner, O. Mandel, T. Esslinger, T. W. Heanch, and I. Bloch, *Nature* **415**, 39 (2002); M. Greiner, O. Mandel, T. W. Heanch, and I. Bloch, *Nature* **419**, 51 (2002).
  - [3] O. Mandel, M. Greiner, A. Widera, T. Rom, T. W. Heanch, and I. Bloch, *Nature* **425**, 937 (2003).
  - [4] D. Jaksch, H.-J. Briegel, J. I. Cirac, C. W. Gardiner, and P. Zoller, *Phys. Rev. Lett.* **82**, 1975 (1999).
  - [5] G. K. Brennen, C. M. Caves, P. S. Jessen, and I. H. Deutsch, *Phys. Rev. Lett.* **82**, 1060 (1999).
  - [6] A. Kay and J. K. Pachos, [quant-ph/0406073](https://arxiv.org/abs/quant-ph/0406073).
  - [7] J. Mompert, K. Eckert, W. Ertmer, G. Birkl, and M. Lewenstein, *Phys. Rev. Lett.* **90**, 147901 (2003).
  - [8] D. Jaksch, C. Bruder, J. I. Cirac, C.W. Gardiner, and P. Zoller, *Phys. Rev. Lett.* **81**, 3108 (1998).
  - [9] A. B. Kuklov, and B. V. Svistunov, *Phys. Rev. Lett.* **90**, 100401 (2003).
  - [10] D. Jaksch, and P. Zoller, *New Journal Phys.* **5**, 56.1 (2003).
  - [11] L. M. Duan, E. Demler, and M. D. Lukin, *Phys. Rev. Lett.* **91**, 090402 (2003).
  - [12] A. Mizel, and D. A. Lidar, [cond-mat/0302018](https://arxiv.org/abs/cond-mat/0302018).
  - [13] P. Rabl, A. J. Daley, P. O. Fedichev, J. I. Cirac, P. Zoller, [cond-mat/0304026](https://arxiv.org/abs/cond-mat/0304026).
  - [14] S. E. Sklarz, I. Friedler, D. J. Tannor, Y. B. Band, C. J. Williams, *Phys. Rev. A* **66**, 053620 (2002).
  - [15] D. C. Roberts and K. Burnett, *Phys. Rev. Lett.* **90**, 150401 (2003).
  - [16] J. K. Pachos, and M. B. Plenio, to appear in *Phys. Rev. Lett.*, [quant-ph/0401106](https://arxiv.org/abs/quant-ph/0401106).
  - [17] S. Sachdev, *Quantum Phase Transitions*, Cambridge University Press (1999).
  - [18] P. Fendley, K. Sengupta, and S. Sachdev, *Phys. Rev. B* **69**, 075106 (2004).
  - [19] K. A. Penson, J. M. Debierre, and L. Turban, *Phys. Rev. B* **37**, 7884 (1988).
  - [20] F. Iglói, *Phys. Rev. B* **40**, 2362 (1989).
  - [21] P. Fendley, K. Sengupta, and S. Sachdev, [cond-mat/0309438](https://arxiv.org/abs/cond-mat/0309438).
  - [22] L. Turban, *J. Phys. C: Solid State Phys.* **15**, L65 (1982).
  - [23] K. A. Penson, R. Jullien, and P. Pfeuty, *Phys. Rev. B*

- 26**, 6334 (1982).
- [24] F. Iglói, J. Phys. A: Math. Gen. **20**, 5319 (1987).
- [25] J. Christiaan, A. d'Auriac, and F. Iglói, Phys. Rev. E **58**, 241 (1998).
- [26] R. B. Laughlin, Science **242**, 525 (1988).
- [27] J. K. Pachos, and P. L. Knight, Phys. Rev. Lett. **91**, 107902 (2003).
- [28] J. K. Pachos and E. Rico, quant-ph/0404048.
- [29] S. Inouye, M. R. Andrews, J. Stenger, H.-J. Miesner, D. M. Stamper-Kurn, and W. Ketterle, Nature **392**, 151 (1998).
- [30] A. Donley, N. R. Claussen, S. L. Cornish, J. L. Roberts, E. A. Cornell, and C. E. Wieman, Nature **412**, 295 (2001).
- [31] S. J. J. M. F. Kokkelmans, and M. J. Holland, Phys. Rev. Lett. **89**, 180401 (2002); T. Koehler, T. Gasenzer, and K. Burnett, cond-mat/0209100.
- [32] W. V. Liu, F. Wilczek, and P. Zoller, cond-mat/0404478.
- [33] A. Kitaev (unpublished).
- [34] For an alternative method see, e.g. [10].
- [35] Y. Aharonov, and D. Bohm, Phys. Rev. **115**, 485 (1959).
- [36] J. K. Pachos, cond-mat/0405374.
- [37] S. L. Cornish *et al.*, Phys. Rev. Lett. **85**, 1795 (2000); J. K. Chin, J. M. Vogels, and W. Ketterle, Phys. Rev. Lett. **90**, 160405 (2003); M. Greiner *et al.*, Phys. Rev. Lett. **92**, 150405 (2004).
- [38] X. G. Wen, F. Wilczek, and A. Zee, Phys. Rev. B **39**, 11413 (1989).
- [39] D. S. Rokhsar, Phys. Rev. Lett. **65**, 1506 (1990).
- [40] D. Sen, and R. Chitra, Phys. Rev. B **51**, 1922 (1995).
- [41] V. Kalmeyer and R. B. Laughlin, Phys. Rev. Lett. **59**, 2095 (1987).
- [42] A. S. Sorensen, E. Demler, and M. D. Lukin, cond-mat/0405079.
- [43] D. A. Huse and M. E. Fisher, Phys. Rev. Lett. **49**, 793 (1982).
- [44] J. I. Latorre, E. Rico, G. Vidal, quant-ph/0304098.
- [45] F. Verstraete, M. Popp, and J. I. Cirac, Phys. Rev. Lett. **92**, 027901 (2004).
- [46] F. Verstraete, M.-A. Matrin-Delgado, Phys. Rev. Lett. **92**, 087201 (2004).
- [47] F. Verstraete, and J.I. Cirac, quant-ph/0311130.
- [48] R. Raussendorf, *et al.*, Phys. Rev. A **68**, 022312 (2003)
- [49] In contrast to Hamiltonian eqn (6.3) the two-spin system  $H = \sum_i -\sigma_i^x \sigma_{i+1}^x$  does not exhibit a finite gap for an infinite chain and possesses a two-fold degenerate ground state. As a consequence the ground state will not be stable (see eg G. Gallavotti, *Statistical Mechanics: A Short Treatise*, Springer 1999).
- [50] E. Barouch and B.M. McCoy, Phys. Rev. A **3**, 786 (1971).
- [51] J. Eisert and M.B. Plenio, J. Mod. Opt. **46**, 145 (1999); J. Eisert (PhD thesis, Potsdam, February 2001); G. Vidal and R.F. Werner, Phys. Rev. A **65**, 032314 (2002); K. Audenaert, M.B. Plenio, and J. Eisert, Phys. Rev. Lett. **90**, 027901 (2003).
- [52] M.B. Plenio and V. Vedral, Contemp. Phys. **39**, 431 (1998); J. Eisert and M.B. Plenio, Int. J. Quant. Inf. **1**, 479 (2003).
- [53] S. C. Benjamin, Phys Rev A **61**, 020301 (2000).
- [54] S. C. Benjamin, Phys. Rev. Lett., **88**, 017904 (2002).
- [55] S. C. Benjamin and A. Brigid, quant-ph/0308113.
- [56] S. C. Benjamin, quant-ph/0104117.
- [57] T. Calarco, U. Dornier, P. Julienne, C. Williams, and P. Zoller, quant-ph/0403197.
- [58] S. Peile, J. V. Porto, B. Laburthe, J. M. Obrecht, B. E. King, M. Subbotin, S. L. Rolston and W. D. Phillips, Phys. Rev. A, **67**, 051603(2003).
- [59] G. M. Palma, K. A. Suominen and A. K. Ekert, Proc. R. Soc. A, **452**, 567 (1996).
- [60] M.B. Plenio, V. Vedral and P.L. Knight, Phys. Rev. A **55**, 67 (1997).
- [61] A. M. Steane, Phys. Rev. Lett. **77**, 793 (1996).
- [62] A. M. Steane, quant-ph/9809054.
- [63] D. Aharonov and M. Ben-Or, quant-ph/9906129.